

Controlled Microwave Module for the Noncontact Measurement of Nonequilibrium Carrier Lifetime in Semiconductors

V. M. Vladimirov, V. G. Konnov, V. V. Markov, N. S. Repin, and V. N. Shepov

Krasnoyarsk Scientific Center, Siberian Branch, Russian Academy of Sciences, Russia

e-mail: vlad@ksc.krasn.ru

Received October 22, 2010

Abstract—An original controlled microwave module for the noncontact measurement of the parameters of semiconductors is briefly described. The module allows automatic control of frequency, amplitude, Q factor, and the shape of a resonance curve shape of a microwave cavity upon its loading by a measured semiconductor. The results of the measurements of nonequilibrium carrier lifetime in single-crystal and multicrystalline silicon wafers using the microwave module are presented.

DOI: 10.1134/S1063739711020090

INTRODUCTION

A noncontact microwave method of the measurement of nonequilibrium carrier lifetime (NCLT) in semiconductors is long-known [1, 2]. The theory and physical grounds of the method were considered [3–9] and engineering solutions providing the NCLT measurement by the noncontact microwave method were proposed [10–16].

With advances in multicrystalline and single-crystal silicon technology, there appeared a need for a universal noncontact NCLT measuring instrument that would allow measurements within a broader NCLT range, including the ranges for both single-crystal and multicrystalline silicon. In addition, it became necessary to automatize the noncontact microwave method and apply a modern element base allowing a considerable reduction of the dimensions of the measuring equipment. The aforesaid required solving a number of problems.

One of the problems to be solved is the automatic matching of the frequency of the microwave oscillator with the frequency of the microwave cavity, in an electric field antinode of which a measured semiconductor is placed. Matching must be attained in a wide range of semiconductor resistivities, including the values characteristic of multicrystalline and single-crystal silicon. To adjust multisilicon technology, it is often required to measure the NCLT from 0.1 μs on specimens with a resistivity spread from 0.1 to 10 $\Omega\text{ cm}$. At the same time, in order to control the single-crystal silicon NCLT, a measuring instrument should measure the NCLT in the millisecond range on specimens with resistivity over 1000 $\Omega\text{ cm}$.

In the first meters, the microwave oscillators were based, as a rule, on Gunn diodes. The microwave cavities were based on waveguide transmission lines. The microwave cavity was connected with a measured semiconductor specimen via either an aperture in a

waveguide wall [10–13] or an inductive post in the evanescent waveguide [14–16]. The frequencies were matched manually with an adjusting screw [10, 11, 14–16]. Such an engineering solution made further automation of the NCLT measurements difficult.

Application of self-excited oscillator (SEO) circuits for the noncontact microwave NCLT measurements [17] allow automatic control of frequency and the minimum value of the microwave power reflected from a semiconductor. However, they do not allow controlling the shape of the resonance curve, which is required at the NCLT measurements on low-resistance semiconductor specimens. During the NCLT measurements on such specimens, the Q factor of the microwave cavity main mode on which the measurements are performed substantially decreases, which causes instability of the SEO operation. For this reason, for the noncontact microwave NCLT measurements, a circuit with a controlled SEO frequency scan with further visualization of the resonance curve is preferable [18, 19]. Such a solution makes it possible to control the Q factor of the semiconductor-loaded microwave cavity and eliminate distortions in the resonance line to enhance the accuracy of the NCLT measurements.

Another problem arising during automation of the noncontact microwave NCLT measurements on semiconductors is caused by a considerable difference both in the levels of the microwave powers reflected from the low- and high-resistance semiconductor specimens and in the variation of these levels under the action of pulse laser radiation on a semiconductor. One of the ways of solving this problem is using the NCLT measurements method of passing microwave power on high-resistance specimens and the method of reflected microwave power on low-resistance ones [20].

In this study, measurements in wide NCLT and resistivity ranges of silicon by the reflected microwave

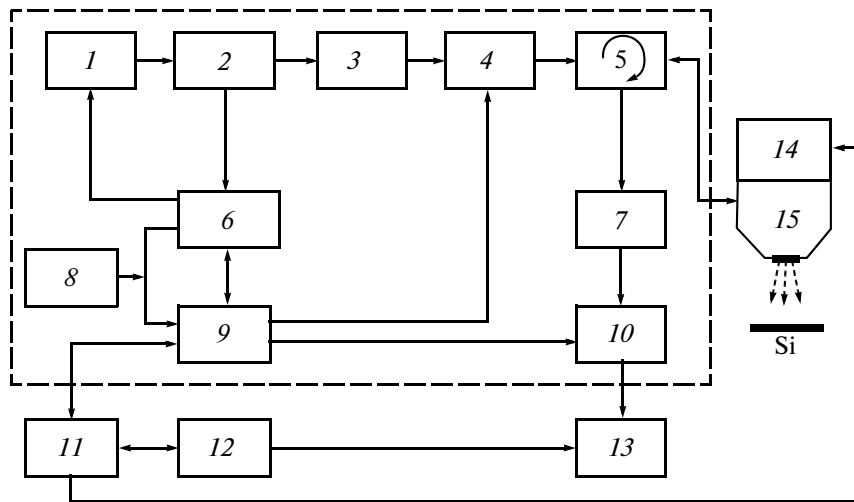


Fig. 1. Block diagram of the meter: (1) voltage-controlled oscillator (VCO), (2) power divider, (3) microwave amplifier, (4) controlled attenuator, (5) circulator, (6) frequency synthesizer, (7) power sensor, (8) reference oscillator, (9) programmable logic integrated circuit, (10) operational amplifier, (11) control card, (12) personal computer, (13) ADC, (14) laser diode, and (15) microwave cavity.

power are proposed to be performed using a special microwave cavity design, which is highly sensitive to minor variations in the microwave power reflected from a semiconductor [21].

The aim of this study is to develop a controlled microwave module for an automatic meter of the NCLT in multicrystalline and single-crystal silicon wafers by the noncontact microwave method. The measurements should be performed in a single reflectance mode.

PRINCIPLE OF THE MICROWAVE MODULE'S OPERATION

Figure 1 shows a block diagram of the meter. The dashed line indicates the composition of the microwave module designed on the principle of digital phase automatic control of the frequency of a voltage-controlled oscillator (VCO).

The microwave module operates as follows. A control program command from PC 12 is translated to control card 11 via a USB port. The card controller coordinates the operation of a programmable logic integrated circuit (PLIC) 9 and the laser-diode radiation control circuit. The programmable logic integrated circuit controls the operation of frequency synthesizer circuit 6, digital attenuator 4, and operational amplifier 10.

Voltage-controlled oscillator 1 forms a microwave signal (F_s) within the frequency range of 4800 to 5300 MHz. The microwave signal from the VCO is supplied to power divider 2, from which a part of the signal is supplied to a two-stage microwave amplifier 3 and the rest of the signal is supplied to digital frequency synthesizer 6. A signal with a frequency of 100 MHz from reference generator (F_{ref}) 8 is supplied to the other input of the synthesizer.

The comparison frequency F_s/N and F_{ref}/n is 100 kHz. Frequency division is implemented by built-in frequency dividers; N is the variable (controlled) division coefficient and n is the constant one.

At the output of the phase frequency detector (PFD) included in the frequency synthesizer, a control signal forms depending on the difference of the phases of the compared signals F_s/N and F_{ref}/n . Voltage from the PFD output is supplied to the VCO via a dc amplifier and a low-pass filter and stabilizes the specified frequency.

From the output of amplifier 3, the microwave power is supplied to controlled attenuator 4 and, then, via circulator 5 to microwave cavity 15 loaded by a measured semiconductor specimen. To perform the NCLT measurements in the wide silicon resistivity range, the microwave's power can be varied within 0.01–100 mW with the digital attenuator.

The microwave signal reflected from the semiconductor is supplied to power sensor 7 via circulator 5. Then, the detected signal is amplified by operational amplifier 10 with a controlled gain. Using a serial code from the PLIC, the gain can be varied from 1 to 20, which provides amplification of the information signal up to the level required for operation of 12-bit analog-to-digital converter (ADC) 13. The maximum ADC discretization frequency is 100 MHz and the memory buffer volume is 1024 kwords. These parameters of the ADC allow measuring the entire curve of the photoconductivity decay per laser radiation pulse even at NCLT values of about 0.1 μ s.

The microwave cavity providing connection of the microwave oscillator with a measured semiconductor specimen is implemented as a microstrip cavity (MSC) operating in the reflectance mode. The topology of the MSC conductor is presented in Fig. 2. The

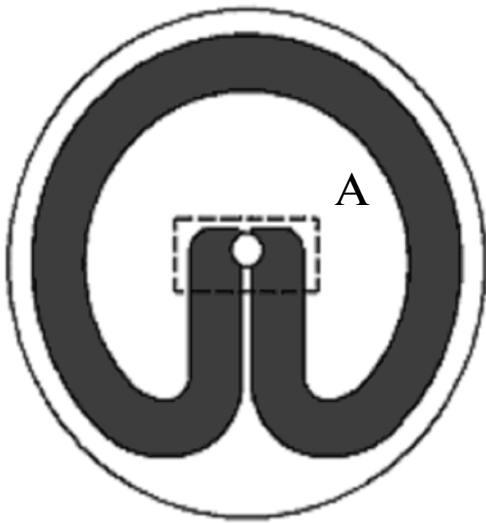


Fig. 2. MSC conductor topology.

opposite ends of the strip conductor, on which antiphase high-frequency electric field antinodes are located, are reunited via a gap [21]. The sensitivity of such a microwave cavity is much higher than that of the cavity reported in [18], which enhances measurement accuracy. This happens because in such a microwave cavity, high-frequency electric field lines are closed not only between the strip conductor and the shield but also between the antiphase ends of the strip conductor that are affected by the measured semiconductor. Between the ends of the strip conductor, there is an aperture via which radiation of the laser diode fixed at the other side of the microwave cavity passes. This region is shown in the figure by the dashed line. The laser diode radiation wavelength is $1.06 \mu\text{m}$ and the limiting power of continuous radiation is 500 mW.

The microwave cavity is designed in such a way that the measured semiconductor does not affect the entire microwave cavity but only its Δ region.

After the optimal connection between the microwave cavity and the measured silicon specimen is established, the laser radiation pulse of a specified length and power passes via the aperture in the cavity by a control program command and excites nonequilibrium carriers in the semiconductor. Photoconductivity decay is detected by means of the time dependence of the microwave cavity's resonance line amplitude. Then, the effective NCLT is determined by a portion of photoconductivity decay and the volumetric NCLT is calculated.

Figure 3 presents the frequency dependences of the microwave power reflected from the microwave cavity loaded by silicon specimens (curves *a* and *b*), where F is the frequency of the signal from the microwave module. The curves correspond to specimens 1 and 2, which are wafers of single-crystal and multicrystalline n silicon with thicknesses of 6 and 3 mm, respectively. The respective resistivity values for specimens 1 and 2 are 2500 and $0.05 \Omega \text{ cm}$. As is seen from the figure, the microwave module with a specially designed microwave cavity allows reliable detection of the reflected microwave power within the silicon resistivity range of 0.05 to $2500 \Omega \text{ cm}$. This range is not limiting for the microwave module.

To observe the resonance line in more detail, the frequency range of the microwave module can be arbitrarily changed within 4800–5300 MHz. The frequency tuning pitch is discrete; its minimum value is 0.1 MHz.

MEASUREMENT RESULTS

Figure 4 shows the measured time dependences of the rise and decay in photoconductivity for specimens 1 (upper picture) and 2 (lower picture). The results for specimen 1 were obtained at a microwave module power of 2 mW, a single laser radiation pulse with a power of 30 mW and a length of $1000 \mu\text{s}$. The results for specimen 2 were obtained at a microwave module power of 80 mW, a laser radiation power of 450 mW, and a pulse length of $50 \mu\text{s}$, with data accumulated from 30 measurements. It is seen that the microwave

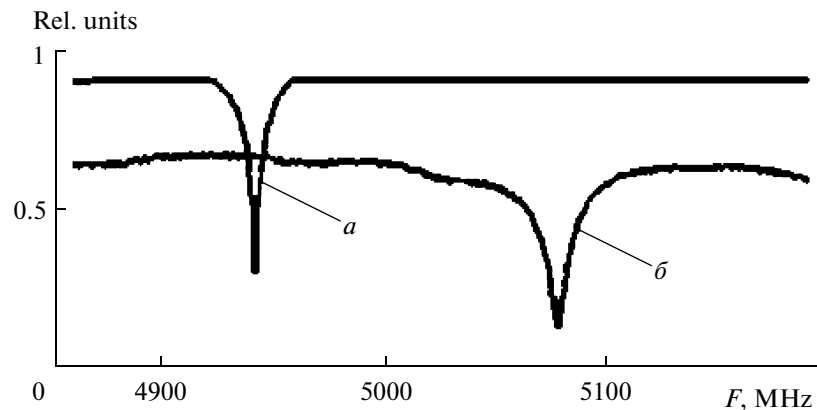


Fig. 3. Frequency dependence of the microwave power reflected from (a) single-crystal and (b) multicrystalline specimens.

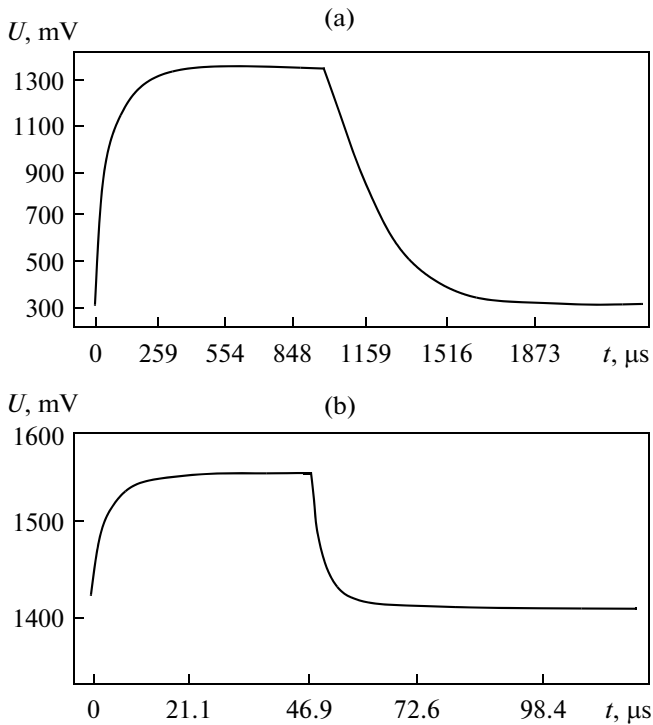


Fig. 4. Time dependences of photoconductivity for specimens (a) 1 and (b) 2.

module with the application of a specially designed microwave cavity allows reliable detection of the photoconductivity' rise and decay curves by the reflected microwave power method.

The control program selects the photoconductivity decay portion in the obtained time dependence of photoconductivity, depending on the chosen standard of experimental data processing. According to the international SEMI MF 1535 standard [22], the effective NCLT is calculated from the lower portion of the photoconductivity decay curve, from 45 to 5% from the point at which the decay starts. According to the SEMI MF 28b standard [23], the upper portion of the photoconductivity decay curve is selected from the point at which the decay starts to the point where the photoconductivity value is smaller by a factor of e . Then, the experimental points in the selected portion of the curve are approximated by the exponential dependence. The control program also allows manual selection of an arbitrary portion of the photoconductivity decay curve for its further approximation.

The time dependence of the photoconductivity decay at a laser radiation pulse length that is sufficient for attaining a uniform concentration of nonequilibrium carriers in a semiconductor can be approximated as [5]

$$U = ce^{t/\tau_{eff}} + \text{const}, \quad (1)$$

where τ_{eff} is the effective NCLT, t is the time coordinate, U is the photoconductivity decay value, c is the calibration coefficient, and const is the constant

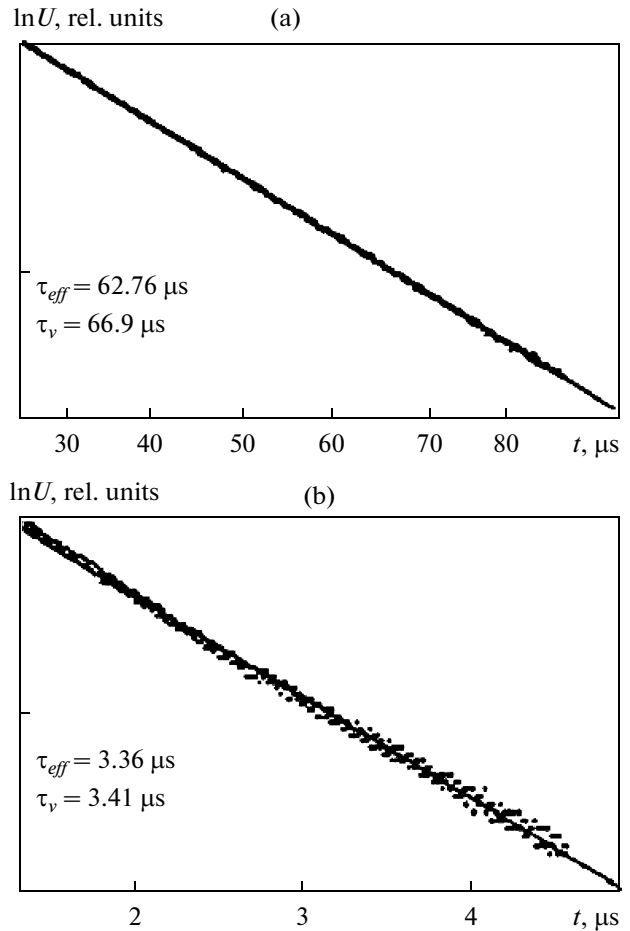


Fig. 5. Results of the measurements of effective, and calculations of volumetric NCLTs for specimens (a) 1 and (b) 2.

determined by the level of the reflected microwave power in the absence of laser diode radiation. This constant is dependent on the resistivity of a semiconductor and independent of photoconductivity.

The volumetric NCLT is related to the effective one as [5]

$$\frac{1}{\tau_v} = \left(\frac{1}{\tau_{eff}} - \frac{1}{\tau_s} \right), \quad (2)$$

where τ_v is the volumetric NCLT and τ_s is the surface recombination time. The surface recombination contribution can be divided into two components: diffusion and its own surface recombination:

$$\tau_s = \tau_{diff} + \tau_{sr} = \frac{d^2}{\pi^2 D} + \frac{d}{2S}, \quad (3)$$

where d is the specimen thickness, π is the constant, S is the rate of the NC surface's recombination, and D is the NC diffusion coefficient.

For our specimens with an unpolished surface, the rate of surface recombination exceeds 10 000 cm/s. Since the respective thicknesses of our single-crystal and multi-

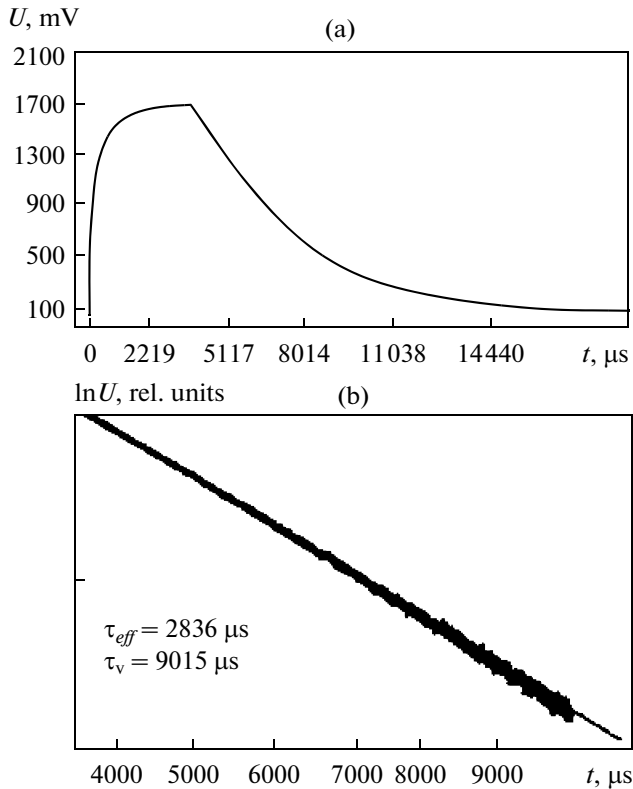


Fig. 6. (a) Rise and decay photoconductivity curve and (b) results of the measurements of effective, and calculation of volumetric, NCLTs for a single-crystal silicon specimen with the millisecond NCLT.

crystalline silicon specimens are 6 and 3 mm, respectively, the contribution of the second term in formula (3) is negligible. Therefore, during experimental data processing, the NCLT was calculated by the formula

$$\tau_v = \left(\frac{1}{\tau_{eff}} - \frac{\pi^2 D}{d^2} \right)^{-1}, \quad (4)$$

where the effective NCLT is determined from formula (1).

Figure 5 presents the measured effective NCLT and the volumetric NCLT calculated by formula (4) for specimens 1 and 2 approximated by the SEMI MF 28b standard, where t is the photoconductivity decay time and $\ln U$ is the photoconductivity's amplitude logarithm. The difference between the effective and volumetric NCLTs is minor due to large specimen thicknesses (6 mm for the single-crystal and 3 mm for the multicrystalline silicon).

Figure 6 shows the measured time dependence of photoconductivity (a) and the measured NCLTs for the 7-mm-thick single-crystal p silicon with a resistivity of $1000 \Omega \text{ cm}$. One can see that the microwave module allows reliable detection of the NCLT in the millisecond range.

CONCLUSIONS

The microwave module is fabricated by microstrip technology in a dust- and moisture-proof casing. Its dimensions are $150 \times 80 \times 30 \text{ mm}$. The maximum frequency tuning range of the microwave module is 4800–5300 MHz with a minimum pitch of 0.1 MHz. The power tuning range is 0.01–100 mW.

The developed microwave module allows automatic NCLT measurements on the single-crystal and multicrystalline silicon wafers in a wide range of resistivities. The measurements are performed by the reflected microwave power using the noncontact method.

The microwave module makes it possible to measure the NCLT not only at the frequency of the reflected microwave power, but also at an arbitrary frequency of this frequency range. The measurements of the NCLT at the slope of the resonance curve and by the change in the resonance line width become feasible. In addition, controlling the resonance line shape allows eliminating the distortions of the resonance line during the NCLT measurements, thus enhancing their accuracy.

On the basis of the microwave module and the measurement table displacement controller used in the automatic meter of the resistivity of silicon wafers and ingots [24], a Taumetr 2M device was developed for the measurements of the NCLT in silicon by the noncontact microwave method.

ACKNOWLEDGMENTS

This study was supported by the Importozameshchenie Program of the Siberian Branch of the Russian Academy of Sciences.

REFERENCES

1. Ramsa, A.P., Jacobs, H., and Brand F.M., *J. Appl. Phys.*, 1959, vol. 30, no. 7, p. 1054.
2. Deb, S. and Nag, B.R., *J. Appl. Phys.*, 1962, vol. 33, no. 4, p. 1604.
3. Jacobs, H., Brand, F.M., Meindl, J.D, et al., *TIRI*, 1963, vol. 51, no. 4, p. 608.
4. Kunst, M. and Beck, G., *J. Appl. Phys.*, 1988, vol. 63, no. 4, p. 1093.
5. Pavlov, L.P., *Metody izmereniya parametrov poluprovodnikov materialov* (Methods of the Measurements of the Parameters of Semiconductor Materials), Moscow: Vysshaya shkola, 1987.
6. Sanders, A. and Kunst, M., *Sol. St. Electron.*, 1991, vol. 34, p. 1007.
7. Swiatkowski, C., Sanders, A., Buhre, K.-D., and Kunst, M., *J. Appl. Phys.*, 1995, vol. 78, no. 3, p. 1763.
8. Schofthaler, M. and Brendel, R., *J. Appl. Phys.*, 1995, vol. 77, no. 7, p. 3162.
9. Schmidt, J. and Aberle, A.G., *J. Appl. Phys.*, 1997, vol. 81, no. 9, p. 6186.
10. Thomas, A., Kennedy, Jr., and McCombe, B.D., US Patent 4087745, 1978.

11. Tributsch, H., Beck, G., and Kunst, M., US Patent 4704576, 1987.
12. Kawata, Y., Kusaka, T., Hashizume, H., and Futoshi, M., US Patent 5438276, 1995.
13. Yoshida, N., Takamatsu, H., Sumie, S., et al., US Patent 5760597, 1998.
14. Danilov, G.N., Medvedev, Yu.V., and Petrov, A.S., USSR Inventor's Certificate no. 347691, 1972.
15. Nalivaiko, B.A., USSR Inventor's Certificate no. 496515, 1975.
16. Akhmanaev, V.V., Danilov, G.N., Medvedev, Yu.V., and Petrov, A.S., RF Patent no. 1212156, 1994.
17. Goryunov, N.N., Kobeleva, S.P., Charykov, N.A., et al., *Zavodskaya laboratoriya. Diagnostika materialov*, 2004, vol. 70, no. 5, p. 27.
18. Boda, J., Ferenczi, G., Horvath, P., et al., US Patent 5406214, 1995.
19. Vladimirov, V.M., Konnov, V.G., Markov V.V., et al., Microwave Module for Noncontact Measurements of the Parameters of Semiconductors, *Trudy 20-oi mezh-*
dunarodnoi Krymskoi konferentsii po SVCh tekhnike i telekommunikatsionnym tekhnologiyam (Proc. 20th Int. Conf on Microwave Engineering and Telecommu-
nical Technology), Sevastopol', 2010, p. 967.
20. Borodovskii, P.A., Buldygin, A.F., and Tokarev, A.S., *Fiz, Tekh. Poluprovodn.*, 2004, vol. 38, no. 9, p. 1043.
21. Vladimirov, V.M., Markov, V.V., Martynovskii, V.N., and Shepov, V.N., RF Patent no. 2010104582/07, 2010 (unpublished).
22. SEMI MF1535. Test Methods for Carrier Recombination Lifetime in Silicon Wafers by Noncontact Measurement of Photoconductivity Decay by Microwave Reflectance.
23. SEMI MF28(b). Standard Test Methods for Minority-Carrier Lifetime in Bulk Germanium and Silicon by Noncontact Measurement of Photoconductivity Decay by Microwave Reflectance.
24. Vladimirov, V.M., Grinin, E.F., Sergii, M.E., and Shepov, V.N., *Izm. Tekh.*, 2010, no. 5, p. 51.